Water Research 83 (2015) 227–236

Contents lists available at ScienceDirect

Water Research

journal homepage: www.elsevier.com/locate/watres

A hydrodynamics-based approach to evaluating the risk of waterborne pathogens entering drinking water intakes in a large, stratified lake

Andrea B. Hoyer [a, *], S. Geoffrey Schladow [c, d], Francisco J. Rueda [a, b]

[a] Water Research Institute, University of Granada, C/ Ramón y Cajal 4, 18071 Granada, Spain
[b] Department of Civil Engineering, University of Granada, Campus Universitario de Fuentenueva (Edificio, Politécnico), 18071 Granada, Spain
[c] Department of Civil and Environmental Engineering, University of California, Davis, One Shields Avenue, Davis, CA 95616, USA
[d] Tahoe Environmental Research Center, University of California, Davis, 291 Country Club Dr., Incline Village, NV 89451, USA

ARTICLE INFO

Article history:
Received 7 October 2014
Received in revised form
23 March 2015
Accepted 8 June 2015
Available online 20 June 2015

Keywords:
Drinking water contamination
Body-contact recreation
Individual-based model
Back-tracking algorithm
UV inactivation
Cryptosporidium

ABSTRACT

Pathogen contamination of drinking water lakes and reservoirs is a severe threat to human health worldwide. A major source of pathogens in surface sources of drinking waters is from body-contact recreation in the water body. However, dispersion pathways of human waterborne pathogens from recreational beaches, where body-contact recreation is known to occur to drinking water intakes, and the associated risk of pathogens entering the drinking water supply remain largely undocumented. A high spatial resolution, three-dimensional hydrodynamic and particle tracking modeling approach has been developed to analyze the risk and mechanisms presented by pathogen dispersion. The pathogen model represents the processes of particle release, transport and survival. Here survival is a function of both water temperature and cumulative exposure to ultraviolet (UV) radiation. Pathogen transport is simulated using a novel and computationally efficient technique of tracking particle trajectories backwards, from a drinking water intake toward their source areas. The model has been applied to a large, alpine lake – Lake Tahoe, CA–NV (USA). The dispersion model results reveal that for this particular lake (1) the risk of human waterborne pathogens to enter drinking water intakes is low, but significant; (2) this risk is strongly related to the depth of the thermocline in relation to the depth of the intake; (3) the risk increases with the seasonal deepening of the surface mixed layer; and (4) the risk increases at night when the surface mixed layer deepens through convective mixing and inactivation by UV radiation is eliminated. While these risk factors will quantitatively vary in different lakes, these same mechanisms will govern the process of transport of pathogens.

1. Introduction

Pathogen contamination of aquatic ecosystems is a severe threat to human health worldwide (Sherchand, 2012). Even in developed countries, the risk of pathogen contamination is significant. The protozoan parasites *Cryptosporidium* spp. and *Giardia* spp., or rather their (oo)cysts, are widespread in lakes and reservoirs (Jellison et al., 2002; Brookes et al., 2004a). In the US, the presence of *Cryptosporidium parvum* is estimated to occur in 55% of surface waters and 17% of drinking water supplies (Rose et al., 1991; LeChevallier et al., 1991). The Center for Disease Control (CDC), the U.S. Environmental Protection Agency (USEPA), and the Council of State and Territorial Epidemiologists maintain a collaborative surveillance system for collecting and reporting data about the occurrences and causes of waterborne-disease outbreaks related to drinking water and recreational waters (USEPA, 2002). The Beaches Environmental Assessment of Coastal Health (BEACH) Act (USEPA, 2002; Wade et al., 2006) requires testing recreational beach waters for fecal coliforms (enterococci or *Escherichia coli*) on a weekly basis. In Europe, the Directive 76/160/EEC governs the quality of bathing waters specifying threshold values for microbiological and physicochemical parameters (Council of the European Communities, 1976). Parasites, however, are not monitored on a regular basis. Although indicator organisms, such as enterococci and *E. coli*, are used to monitor pathogens, they are not necessarily indicative on the presence of parasites such as *Cryptosporidium* or *Giardia* (Harwood et al., 2005; Abdelzaher et al., 2010 and references therein).

* Corresponding author.
E-mail addresses: abhoyer@ugr.es (A.B. Hoyer), gschladow@ucdavis.edu (S.G. Schladow), fjrueda@ugr.es (F.J. Rueda).

http://dx.doi.org/10.1016/j.watres.2015.06.014
0043-1354/

The Safe Drinking Water Act currently requires drinking water treatment plants of surface water sources to have the technical capacity to remove 99.9% of *Giardia* cysts (USEPA, 1989). *Cryptosporidium* poses a problem to water treatment as it is highly resistant to conventional methods of disinfection, such as chlorination (Betancourt and Rose, 2004; Standish-Lee and Loboschefsky, 2006; WHO, 2008). The small size and omnipresence of its oocysts has caused many health outbreaks in drinking as well as recreational waters (Craun et al., 2005; Coupe et al., 2006). The most severe outbreak due to the transmission of *Cryptosporidium* through drinking water in Wisconsin in 1993 resulted in 403,000 infected persons (MacKenzie et al., 1994), including lethal cases (Hoxie et al., 1997). The first recreational outbreak of gastrointestinal illness associated with this pathogen (cryptosporidiosis) was reported in 1988 in Los Angeles (CDC, 2000, 2001). Yoder et al. (2004) reported 15 water-borne outbreaks in recreational waters associated with *Cryptosporidium* between 2001 and 2002, in spite of prior water treatment. Cryptosporidiosis inflicts morbidity in healthy people and mortality in children, immune-suppressed individuals and the elderly (Masur et al., 2002; Farthing, 2006; WHO, 2008). Fortunately, a treatment for cryptosporidiosis has been found (Farthing, 2000, Smith and Corcoran, 2004; Rossignol et al., 2006 reported in King and Monis, 2007).

The major source of pathogens in surface sources of drinking waters is human wastes (Gallaher et al., 1989; Rose et al., 2002; Fayer, 2004). A fecal accident by an infected person is the most common cause of recreational water outbreaks (Rose et al., 2002). Empirical studies have demonstrated a positive relationship between bather density and the level of *Cryptosporidium* and *Giardia* (Graczyk et al., 2007; Sunderland et al., 2007). Swimming and other body-contact recreational activities have been identified by the USEPA, California Department of Public Health (DPH) and other public health professionals as a potential source of microbiological contamination of recreational waters. The concentration of shed pathogens in recreational water bodies is of high spatial and temporal variability being greatest in zones associated with body-contact recreation, such as water skiing, jet skiing and swimming, and times of maximal recreational use (Anderson et al., 1998). Anderson et al. (1998) showed that high loads of pathogens due to body-contact recreation may reach drinking water intakes on a regular basis and, thus, constitute a potential risk for disease outbreaks through drinking water supplies. The approach used by Anderson et al. (1998) and Stewart et al. (2002) was based on a relatively simple finite segment model based on a coarse horizontal resolution (500 m $\times$ 500 m segments) and a two-layer vertical grid. For the analysis of pathogens released in near-shore areas, such as recreational beaches, however, a finer spatial resolution is necessary to adequately resolve the complex coastal bathymetry and circulation patterns. While sufficiently high model resolutions were out of reach in the past due to hardware limitations, today they are feasible. Further, Anderson et al. (1998) considered pathogens inactivation due to temperature only. Laboratory and field studies have shown that *Cryptosporidium* is highly sensitive to ambient UV radiation (Rochelle et al., 2005; Connelly et al., 2007; King et al., 2008).

Our goal is to assess the probability or risk of viable/infectious human intestinal pathogens, focusing on *Cryptosporidium* as an example, released at beach areas to enter a drinking water intake. In contrast to previous studies on the risk assessment, the present work is based on a time-varying, high spatial resolution, three-dimensional (3D) hydrodynamic model. Model resolution in the horizontal plane was 20 m $\times$ 20 m, and as small as 0.5 m in the vertical. As well as predicting the transport and dispersion of particles (viz., pathogens) the model integrates the exposure to temperature and UV radiation experienced by all the particles. Lake Tahoe is used as a test case. It is a large, ultra-oligotrophic, subalpine lake well known for its clear, blue water. In addition to its use for recreation, Lake Tahoe serves as a source of unfiltered drinking water.

The results are based on the particle transport and dispersion model proposed by Hoyer et al. (2014), but extended for the case of pathogen transport. A novel technique of back-tracking pathogens trajectories is used which allows for studying non-point contamination at a modest computational cost. This technique provides a very direct way to represent the likely transport of pathogens to water intakes from near-shore areas where body-contact recreation is occurring. Several key issues are addressed in this work. First, we present the pathogen dispersion model. Next, we determine the sources of pathogens entering drinking a water intake and the pathogens' pathways of migration. Based on these pathways, we quantify the environmental stressors (i.e. temperature and light) the pathogens are exposed to during their journey. Finally, we evaluate the likelihood of survival of pathogens, and determine the probability of pathogen withdrawal to identify potential periods of drinking water contamination.

2. Methods

2.1. Approach

A 3D Lagrangian, individual-based particle model developed by Hoyer et al. (2014) was modified to assess the risk of pathogens entering the drinking water supply from intakes in a lake, hereafter referred to as the pathogen model. These simulations are driven by lake current and turbulence simulations conducted with a 3D hydrodynamic model. Unlike the conventional approach where pathogens are tracked from a point of origin, the velocity fields are inverted and the points of origin of individual pathogens are calculated by back-tracking their individual trajectories from the area of withdrawal.

This technique is computationally efficient. The non-point source nature of pathogens released by body-contact recreation would require a large number of simulations from different beach areas, containing many potential points of origin. In contrast, the knowledge of the point of concern (water intake) makes it possible to consider only those (simulated) pathogens originating from sources areas (recreational beaches) that reach the water intake. In the following, the term ‘particles’ refers to all individual particles simulated by the model, while ‘pathogens’ are those particles that were predicted to origin from recreational beaches. The validation of the hydrodynamic model has been previously described (Hoyer et al., 2015). The simulation results permitted the establishment of risk patterns, their temporal variations and the link existing between risk and local lake circulation and stratification dynamics. Although this study focuses on *Cryptosporidium*, the generic pathogen dispersion model may be applied to any other pathogen, such as for example *Giardia* spp., as well as bacteria and viruses. Likewise, Lake Tahoe is taken here as a study case, while the model is readily applicable to any water body.

2.2. Pathogen model

The pathogen model consists of a Release-module, a Transport-module and a Survival-module. The modules run sequentially and independently of each other. The model is driven by external computations that simulate hydrodynamic conditions prevailing in the lake. A Cartesian grid forms the domain for all simulations. A detailed description of the original dispersion model and the links between the different modules and external computations can be found in Hoyer et al. (2014).

The **R**elease–module (or R-module) simulates the process of pathogen release into the water column by body-contact recreation. Pathogens may be released from skin surface during contact with water (shedding) and through accidental fecal release (AFR). The probability of pathogen release P_R is given by the prevalence rate R_P, that is, the fraction of recreators infected by *Cryptosporidium*. This approach predicts the upper limits of the risk of pathogen release, given the underlying assumption (for simplicity) that all particles released per infected recreator are infectious and of the same hydrodynamic characteristics (surface charge and settling velocity) as *Cryptosporidium*. Note that the recreator density is taken to above zero, $C_R > 0$ ind $m^{-2}d^{-1}$, at all days during the study period (even on cloudy days), but that the risk of pathogen contamination becomes zero for $R_P = 0$. Pathogen release was assumed to occur during the day by recreators and during nighttime from the sediments through resuspension (Wu et al., 2009; Abdelzaher et al., 2010). The solution of the module consists of a time series of number of pathogens released into the pelagic over a given time period *tl*.

The **T**ransport-module (or T-module) simulates the pathways of released pathogens between beach areas and water intakes. Time varying 3D velocity fields and vertical diffusivity profiles from the external hydrodynamic computations are the drivers of these simulations. The simulations of the T-module are carried out using a Lagrangian model. In this model, particles are free to move independently of the model grid. However, the underlying hydrodynamic information (i.e. 3D velocity field, vertical eddy diffusivity, and temperature) is provided as input to the model based on the Cartesian grid and then interpolated to the particle position. For a detailed description of the 3D time-varying particle tracking model see Rueda et al. (2008). Pathogens are treated as free particles in accordance with their strongly negative surface charge (at neutral pH) and their resistance to form aggregates with natural soil particles (Ongerth and Pecoraro, 1996; Dai and Boll, 2003; Dai et al., 2004) or organic particles (Brookes et al., 2004b). Particles are back-tracked from the intake to their points of origin. This backdispersion method comprises calculating the particle displacement at each time step from (a) the inverted 3D velocity field and (b) a random component representing the effect of horizontal and vertical diffusion (Han et al., 2005). Transport simulations start every Δt_0 with the release of N_0 particles, from the source cell (i_0, j_0) at time t_0, tracked during a period of ΔT. Pathogens infectivity is sensitive to UV solar radiation (Betancourt and Rose, 2004, and references therein). The most energetic and damaging part of the UV spectrum, UV-B radiation (290–315 nm), is approximately 1% of the global radiation (Grant et al., 1997). The UV-B radiation reaching a given individual l at time t is calculated from its vertical position $z(l, t)$, below the surface, and from the incident short wave radiation reaching the free surface $I_0(t)$ (W m^{-2}), as follows,

$$I(l,t) = 0.01 \cdot I_0(t) \cdot \exp[-k_{UV}(t) \cdot z(l,t)] \quad (1)$$

Here $k_{UV}(t)$ is the constant (in time and space) light attenuation. The light dose experienced by the individual l, as it travels, $ID(l, t)$ (Jm^{-2}), is calculated as follows

$$ID(l,t) = \sum_{t_0}^{t} I(l,t) \cdot \Delta t_T \quad (2)$$

Here Δt_T is the time step of the transport module. $ID(l, t)$ is a cumulative variable, and provides a measure of the energy that a given individual may have received, from time t_0 when it was at the intake to the time t it reaches a source beach site (i,j), t_s $(t = t_s)$. The solution of each of these model runs consists of the temporally varying position of the N_0 particles during time interval ΔT and the history of environmental conditions (temperature and solar radiation) that acted on each individual during its journey.

The **S**urvival-module (or S-module) accounts for the survival/inactivation of pathogens during their transport subject to the environmental conditions recorded in the **T**-module. Particles withdrawn at the intake are considered to be pathogens released by recreators if (a) they originate from a swimming beach and (b) if the environmental conditions endured during their journey do not affect their survival (infectivity). Therefore, the probability P_C of a given intake to be contaminated by pathogens released at any beach source B at an instant of time t is expressed as the product of the probability of pathogen release P_R, the probability of pathogen transport from beach areas toward the intake P_T and the probability of survival P_S

$$P_C = P_R \times P_T \times P_S \quad (3)$$

The probability of transport from beach origin toward the intake, P_T, is the fraction of withdrawn particles that originate from any of beach source areas identified by substrate type (sand) and water column depth H. Here H must be lower than or equal to a critical depth H_{cr} ($H \leq H_{cr}$). The probability that a pathogen remains viable or infectious, P_S, in the presence of water temperatures and solar radiation endured is expressed as

$$P_S = P_\theta \times P_I \quad (4)$$

The probabilities P_θ and P_I correspond to temperature and light, respectively. The probability of survival due to water temperature, P_θ, is calculated from the temperature inactivation rate proposed by Walker and Stedinger (1999).

$$P_\theta = 1 - \left(10^{-2.68} \cdot 10^{0.058\theta}\right) \quad (5)$$

The probability P_θ is evaluated for the mean temperature θ over the time it takes for a given particle to travel from the beach area to the intake. Pathogen inactivation due to solar radiation is defined in terms of infectivity. A given pathogen is considered inactivated when it receives a light dose sufficiently high to inhibit cell division and, hence, infectivity – though it may still be viable (Monis et al., 2014). For simplicity, the light dose necessary to reduce pathogen infectivity to 0.01% (4-log inactivation), ID_{99}, is taken as a critical value and all individuals that receive this dose are deemed to be inactivated. This approach may overestimate the number of infectious pathogens, compared to a probability density function, and may be considered to represent the worst case scenario. The solution of the S-module is a time series of the probability of pathogens to be withdrawn at the intake, calculated every Δt_0 seconds. Here, the pulses of withdrawn pathogens at time t represent the fraction of infectious pathogen originating from recreational beaches. An uncertainty analysis based on Monte Carlo simulations was carried out for one sample day. For the prevalence rate R_P and the light inactivation dose ID_{99}, a total of 10^5 random values was drawn out of the respective ranges 0–0.05 (normal distribution) and 0.7×10^3–3×10^3 Jm^{-2} (log-normal distribution, Table 1). The pathogen contamination P_C was evaluated for each of the parameter sets and the 90%-confidence interval was calculated.

2.3. Application to Cryptosporidium in Lake Tahoe

The pathogen dispersion model was applied to *Cryptosporidium* in Lake Tahoe during a 2 month summer period, from July 1 (day 183) to August 27 (day 240), 2008 (the study period). The location of the drinking water intake and known beach areas that may be potential sources of pathogens to the intake are indicated in Fig. 1b. In spite of reports on different infection rates between children and

Table 1
Model parameters.

Parameter	Symbol	Units	Value/range	Reference
Prevalence rate	R_P	–	0–0.05 ($\mu = 0.025$, $\sigma = 0.01$)	Anderson et al. (1998), Gerba (2000)
Settling rate	w_s	ms^{-1}	10^{-7}	Medema et al. (1998), Dai and Boll (2006)
Light attenuation coefficient	k_{UV}	m^{-1}	0.15	Rose et al. (2009)
Inactivation dose	ID_{99}	Jm^{-2}	0.7×10^3–3×10^3 ($\mu = 10^3$, $\sigma = 10^{0.4}$)	Craik et al. (2001), Morita et al. (2002), Hijnen et al. (2006)
Critical depth	H_{cr}	m	2	–

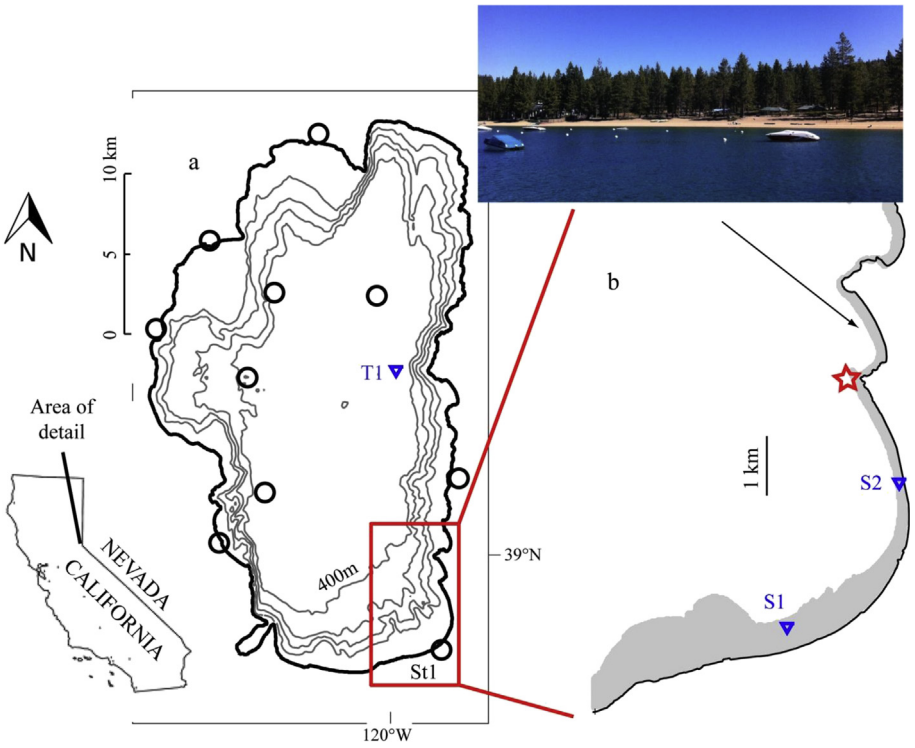

Fig. 1. Lake Tahoe: (a) location, bathymetry (at 100 m intervals) and location of meteorological stations (circles), initial temperature profile (triangle), and (b) area of interest: location of water intake (star), beach areas (shaded gray) and locations of simulated velocity output (triangles).

adults (see Gerba, 2000 and references therein), daily age-structured observations of bathers are difficult to obtain and an average value was utilized. Here two values for the prevalence rate *RP* were evaluated, a mean of 2.5% and maximum of 5% (Anderson et al., 1998; Gerba, 2002). The mean pathogen inactivation dose ID_{99} was 10^3 Jm^{-2}, one order of magnitude higher than values found for UV-C radiation (e.g. Craik et al., 2001; Morita et al., 2002; Hijnen et al., 2006), but in accordance with empirical studies on *Cryptosporidium* inactivation (Rochelle et al., 2005; Connelly et al., 2007; King et al., 2008). In order to evaluate the maximal risk of contamination, a maximum ID_{99} value of 5×10^3 Jm^{-2} was considered together with the maximal prevalence rate ($R_P = 0.05$). The light attenuation coefficient of water k_{UV} was 0.15 m^{-1} at all time (Rose et al., 2009).

The intake was taken to be at a water depth of 15.85 m and 1.8 m above the lake bed. The intake pumping rate was considered continuous at a value of 18 L s^{-1}. Particle releases commenced five days after the beginning of the hydrodynamic simulations, at day 188, to allow the hydrodynamic information to depart from the initial conditions (model spin up). In the T-module, a normal-distributed particle cloud was initialized at the intake on an hourly basis ($\Delta t_0 = 1$ h), centered at the intake with a standard deviation of $\sigma_{xy} = 40$ m (two horizontal grid cells) and $\sigma_z = 0.2$ m in the horizontal and vertical, respectively. The simulated hydrodynamic information (3D velocity field and vertical diffusivity) and temperature was given to the T-module every 3600s ($\Delta t_{h\text{-}output} = 1$ h) and interpolated to Δt_T. Solar radiation data at 10 min intervals was passed to the T-module backward in time to estimate UV exposure and the settling velocity $w_s = 10^{-7}$ m s^{-1} (Yates et al., 1997; Medema et al., 1998; Dai and Boll, 2006) was inverted to become a buoyancy velocity. The number N_0 of particles released in each T-simulation was set to 10^3, to guarantee feasible computational costs. The time step Δt_T was 10s, to satisfy the convergence criterion for particle tracking simulations (Ross and Sharples, 2004) and simulations were run for a time period $T = 1$ d.

2.4. Hydrodynamic simulations

The hydrodynamic simulations of lake currents and mixing variables were carried out using a parallel version of the semi-implicit 3D hydrodynamic model of Smith (2006) (Acosta et al., 2015), and based on the numerical solution of the 3D form of the shallow water equation. The high-resolution hydrodynamic simulations were carried out in a two step nested procedure: In the first step, the whole lake domain was run with low spatial resolution, on a 100 m grid in both the EW and NS directions. This model run produced the boundary conditions for the high resolution simulation. In the second step, these boundary conditions were used to

run a reduced domain of the lake (Fig. 1b) on a 20 m horizontal grid. The vertical resolution was variable, ranging from $\Delta z = 0.5$ m at the surface to $\Delta z = 10$ m near the bottom (i.e. at a depth of 500 m), but maintained the same for both horizontal resolutions. The model was forced using surface heat and momentum fluxes derived from local atmospheric variables (short and long wave radiation, air temperature, relative humidity, and wind speed and direction) observed at 10 locations around the lake (Fig. 1a). The interpolation method proposed by Barnes (1964) was applied to construct the spatially variable wind fields used to force the model. The bathymetry was based on Gardner et al. (1998). The time step of the hydrodynamic model was 50s and 10s for the 100 m and 20 m simulations, respectively. The horizontal eddy diffusivity K_h was estimated based on the horizontal grid resolution and the time step, following Castanedo and Medina (2002), and set to 1 $m^2\ s^{-1}$ (100 m grid) and 0.01 $m^2\ s^{-1}$ (20 m). The initial temperature profile setup a stable stratification obtained from thermistor chain records (T1, Fig. 1a).

3. Results and discussion

3.1. Pathogen sources

A very small percentage (0.02%) of the water withdrawn during the study period was shown to originate from the shallow near-shore beach areas. Withdrawn water originated mainly (99.98%) from a depth below that associated with the shallow beach areas. There were days when 100% of the withdrawal originated from deeper waters, thus, assumed to be free from pathogens. In contrast, in extreme cases, up to 11% of the daily water volume was predicted to come from recreational beaches. Of the pathogens that reached the intake 81% originated from the beaches south of the intake and 19% from beaches north of the intake (Fig. 2). These pathogens were transported by the currents in the coastal boundary layer that is part of a large scale cyclonic (counter-clockwise) gyre at the southern end of the lake (Hoyer et al., 2015).

The near-shore circulation is driven mainly by the local winds acting on the lake surface. Moderate SE and strong SW winds at Timber Cove (Fig. 3) induce persistent and strong northward currents along the south-eastern shore that transport pathogens in the coastal boundary layer from the beach areas towards the intake

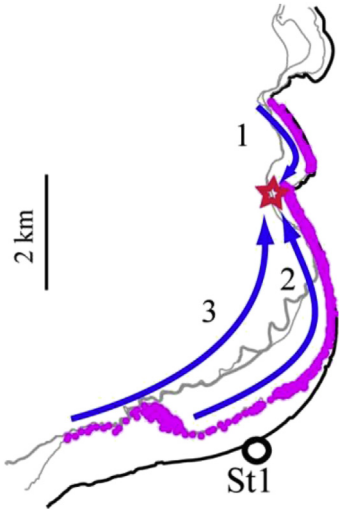

Fig. 2. Distribution of pathogen sources over the study period (dots). The dots correspond to where the back-tracked particles first encountered a beach area. Star marks intake location. Arrows mark pathways of dispersion. Circle marks meteorological station. Depth contours (gray) show 2, 9, and 16 m isobaths for orientation.

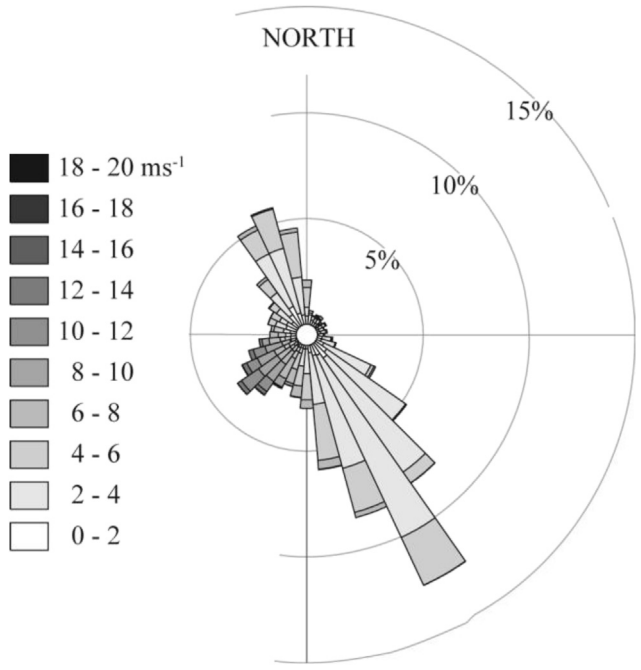

Fig. 3. Observed wind speed and direction at St1 (see Fig. 1a, 2).

(Fig. 4a, b and c). High surface currents (>0.1 m s^{-1}) occurred nearly on a daily basis. Cross-shore currents at the intake were weaker than the alongshore currents, typical for flow in coastal boundary layers (Largier, 2003; Rao and Schwab, 2007; Nickols et al., 2012). The contrast between along-shore and cross-shore currents intensity was predicted also at S2 (Fig. 4b) and at S1 (Fig. 4c). Daily alongshore currents exceeded 0.2 m s^{-1}, while across-shore currents where generally less than 0.05 m s^{-1}. Pathogens originating north of the intake were most likely to be transported to the south during the morning, when winds blew from the NW (onshore winds due to land warming). These winds induced weak to moderate along-shore currents towards the intake (Fig. 4a).

There were three main transportation pathways from the source areas to the intake (Fig. 2): (i) southward along the shoreline of the bay north of the intake, (ii) northward along the south-eastern shore following the 2 m contour, and (iii) northward, from the southern shore across the open water. Transport time from a beach to the intake varied from 1.7 to 24 h depending on the point of origin and the local current velocities. The shortest transport times were observed for pathogens released at the south-eastern beach area (1.7–22.8 h) given its proximity to the intake and the elevated currents generated in the late evening (Fig. 4b). Intermediate transport times were also observed for pathogens originating from beaches north of the intake (6.4–16.9 h), mainly due to its proximity as southward currents were weak (<0.05 m s^{-1}, Fig. 4a). Pathogens released at the southern beach area had the highest range of transport times (2.2–24 h).

3.2. Pathogen withdrawal

Withdrawal of pathogens increased overall during the study period and varied on a daily basis, being highest at night and in the morning (0300–1200). Pulses of pathogens were predicted to enter the intake on a regular basis. We discerned three phases during the study period that varied in the amount and frequency of pathogens arriving at the intake. First the effect of mean values of prevalence rate R_P (=0.025) and inactivation dose ID_{99} (=10^3 Jm^{-2}) on the probability of pathogen contamination was evaluated (Fig. 4d).

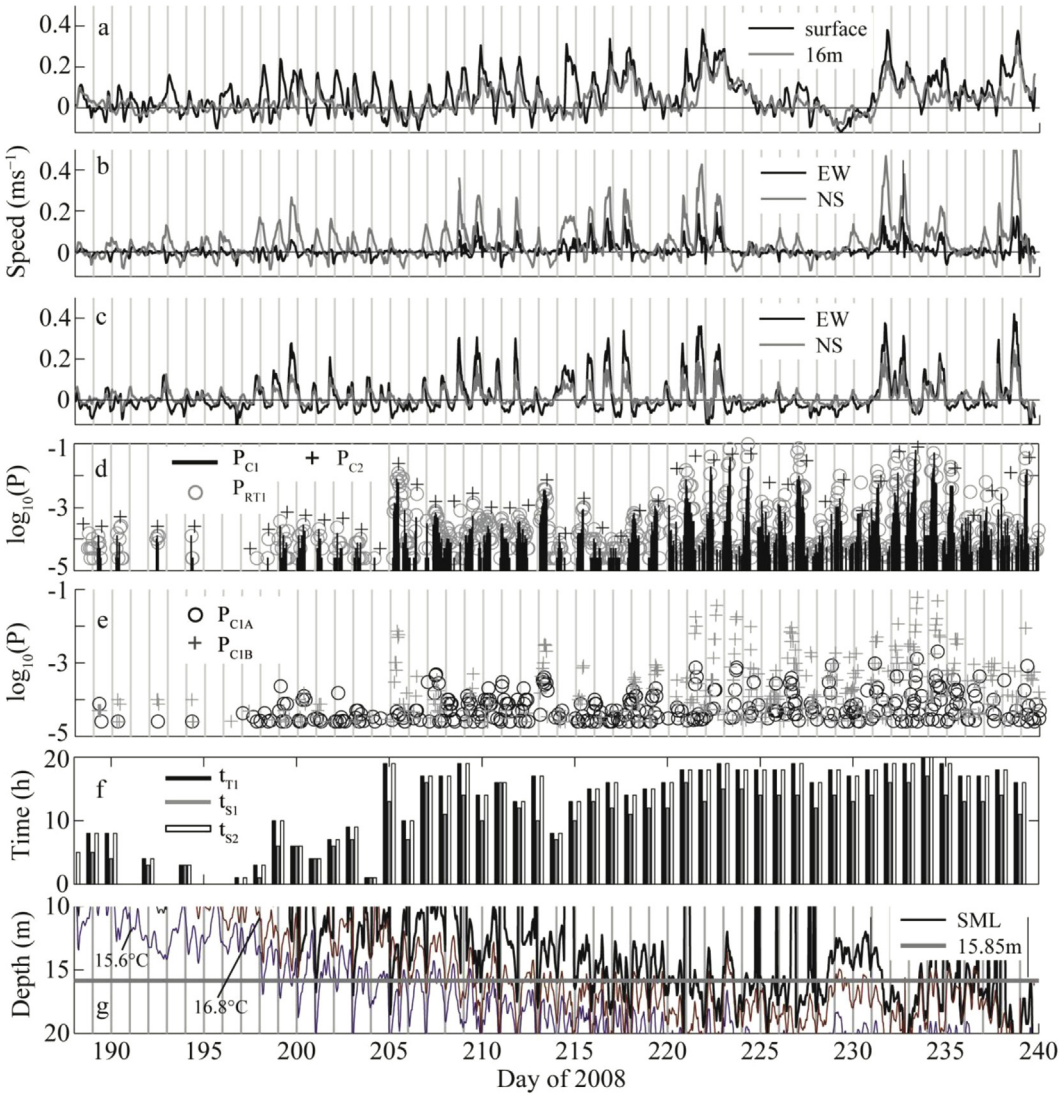

Fig. 4. Time series of current velocities, pathogen withdrawal and surface mixed layer depth. Simulated velocity currents at (a) the intake in the NS direction at the surface (black) and 16 m depth (gray), (b) S2 and (c) S1 in the EW (black) and NS (gray) direction at the surface. North and East are shown as positive. Horizontal line marks zero for reference. (d) Probability of pathogens reaching the water intake for mean values of R_P (=0.025) and ID_{99} (=10^3Jm^{-2}), P_{RT1} (all pathogens) and P_{C1} (viable pathogens); and for maximal values of R_P (=0.05) and ID_{99} (=3×10^3Jm^{-2}), P_{C2} (viable pathogens). Note that P_{C2} is placed at daily noon, independently of hour of daily maximum. (e) Probability of pathogens contamination attributed to direct recreator release P_{C1A} (circles) and attributed to resuspension P_{C1B} (+) for mean values R_P and ID_{99}. (f) Daily time period of pathogen contamination (hours) for mean R_P and ID_{99}, considering all pathogens (t_{T1}) and viable pathogens (t_{S1}); and for maximal R_P and ID_{99}, considering viable pathogens (t_{S2}). (g) Depth of diurnal surface mixed layer (thick black line) calculated from simulated temperature and upper (16.8 °C) and lower (15.6 °C) isotherms of thermocline (thin lines). Horizontal gray line marks depth of intake (z = 15.85 m) and vertical gray bars mark midnight for reference.

During phase 1, from day 188 to day 198, viable pathogens reached the intake episodically with a probability $P_C \leq O(10^{-4})$ during these episodes (Fig. 4d). From day 199 to day 205 (phase 2), withdrawal of pathogens occurred almost on a daily basis with a probability P_C of up to $O(10^{-3})$ during episodes. After day 205 until day 240, (phase 3) pathogens were withdrawn regularly and at significantly higher amounts compared to phases 1 and 2. P_C reached daily maxima of $O(10^{-1})$ during this phase. For maximal values of R_P and ID_{99} (0.05 and 3×10^3 Jm^{-2}, respectively), the daily maxima of pathogen contamination increased and were 2-fold to 15-fold of the daily maxima predicted for the mean values (R_P = 0.025 and $ID_{99} = 10^3$ Jm^{-2}). Note that for minimal values (R_P = 0 and $ID_{99} = 0.7 \times 10^3$ Jm^{-2}), the probability of pathogen contamination P_C become zero (P_C = 0) given that the probability of pathogen release P_R is equal to zero.

The probability of water contamination attributed to pathogens released by recreators P_{C1A} (0800–2000) ranged from $O(10^{-5})$ to $O(10^{-3})$, while contamination by pathogen release attributed to resuspension P_{C1B} (2000–0800) was two orders of magnitude higher, $O(10^{-1})$ (Fig. 4e). Monte Carlo simulations revealed that the 90%-confidence interval for P_C, P_{90}, was zero for P_C = 0 (0100–0500) and narrow from 0600 to 0900 when the median of the pathogen contamination P_{C50} was low ($P_{C50} < 1.5 \times 10^{-3}$), with an average range of 0.4×10^{-3} to 1.8×10^{-3} (Fig. 5). The confidence interval P_{90} increased during the morning hours (1000–1200), when P_{C50} was maximal, with a maximal range at 1200 ($P_{90} = [3 \times 10^{-3}; 1.7 \times 10^{-2}]$). In spite of low P_{C50} during the afternoon, at times the range for P_{90} was also high (e.g. 1400, $P_{90} = [0; 1.0 \times 10^{-2}]$).

Daily time periods of pathogen withdrawal, for R_P = 0.025 and $ID_{99} = 10^3$Jm^{-2}, ranged from 0 to 19 h and 0–14.5 h for total amount of pathogens T_{T1} and active pathogens T_{S1}, respectively (Fig. 4e). For

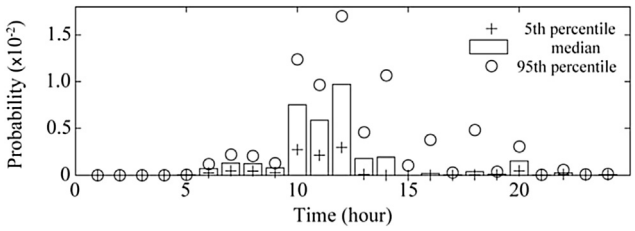

Fig. 5. Probability of pathogen contamination during day 205: 5th percentile (+), median (vertical bars), and 95th percentile (circles).

maximal values of R_P and ID_{99} (0.05 and 3×10^3 Jm^{-2}, respectively), the daily periods of withdrawal of viable pathogens T_{S2} were higher than for the values observed for mean values T_{S1}. However, T_{S2} was equal to T_{T1} given that at least some of the pathogens that reached the intake remained viable at each instance of time Δt_R. Withdrawal of pathogens occurred mainly between 0300 and 1200, with highest values at 1000. Between 0100 and 1000, almost all pathogens that reached the intake were active (or infectious). The highest numbers of inactivated pathogens were withdrawn between 1200 and 1400. The temporal variability of withdrawn pathogens during the day suggests that the pattern of pathogen withdrawal is controlled by the temporal dynamics of vertical dispersion associated with lake motions. The differences between active and inactivated pathogens that reach the intake indicates that indicates that these pathogens are highly sensitive to environmental conditions (temperature or light) endured during their journey toward the intake.

3.3. Pathogen vertical dispersion

The vertical dispersion of pathogens was tightly linked to the temporal dynamics of the depth of the surface mixed layer (SML), over which they are dispersed constantly and uniformly. The thermocline depth of Lake Tahoe ranged from 10 to 20 m during the study period (Fig. 4g) and the stability of the water column was high. The Wedderburn number, W, and the Lake number, L_N, (Stevens and Imberger, 1996), used to parameterize the balance between stabilizing thermal stability and destabilizing wind forcing, were both well above unity at all times. Assuming a two-layer stratification with an upper mixed layer of thickness H, the displacement of the interface, Δh, driven by wind forcing can be estimated as $\Delta h = 0.5H/W$ (Shintani et al., 2010). Interface displacement was of order 8 m, suggesting that the intake at the 16 m isobaths was at times within the SML.

The depth of the diurnal SML ranged between the near surface and the top of the metalimnion due to diurnal temperature variations (Fig. 4g). The SML depth was calculated based on density differences, derived from the simulated temperatures time series at the location of the intake. A threshold value for the base of the SML was assumed to be a density gradient of 0.02 kg m^{-4} (Reynolds, 1984). The depth, at which the density difference $d\sigma$ between the density σ_z and the surface density σ_0 yielded a linear gradient equal to 0.02 kg m^{-4}, was taken to be the depth of the SML. The three phases identified earlier can be related to the maximal depth of the diurnal SML during night time cooling: (i) at the beginning the study period, from day 188 to day 198 (phase 1), the SML was relatively shallow and deepened to a maximal depth of 10 m (Fig. 4g). During phase 2, the maximal depth of the SML during the night increased progressively from 10 m to ~16 m from day 199 to day 205, respectively. After day 205 until day 240 (phase 3), the depth of the SML exceeded 16 m on a daily basis. Consequently, the intake ($z = 15.85$ m) was located at or below the depth of the SML during 80% of the time during this phase. The deepening of the SML below the intake depth exposes the intake to surface (epilimnetic) waters, which are typically of lower water quality and may carry potential contaminants, such as human waterborne pathogens.

The vertical excursions of pathogens from the shallow beach areas to the intake depend on the vertical mixing intensities. *Cryptosporidium* oocysts with a settling velocity $w_s = 10^{-7}$ ms^{-1} (Dai and Boll, 2006) are practically neutrally buoyant in turbulent environments. Vertical eddy diffusivities K_z at the intake were estimated to be of O(10^{-6}) m^2 s^{-1} to O(10^{-2})m^2 s^{-1}(Fig. 6). With a diurnal SML depth H of O(10)m and a minimal K_z of O(10^{-6}) m^2 s^{-1}, as predicted for Lake Tahoe, the vertical eddy velocity v_z ($=K_z/H$) is 10^{-7} m s^{-1} and, thus, of the same order of magnitude as the settling velocity w_s. Even for a settling velocity of O(10^{-6}) m s^{-1}, as reported for *Giardia lambia* cysts (Dai and Boll, 2006), turbulence intensities (indicated by K_z) in the SML of Lake Tahoe can keep these pathogens in suspension over an extended period of time.

The back-trajectories of those particles originating from near-shore areas <2 m depth and withdrawn at the intake revealed transport patterns with respect to the vertical particle position (VPP): (i) the VPP changes frequently between the surface and the bottom in the shallow near-shore beach regions and (ii) the VPP increases progressively until it reaches the depth of the intake (Fig. 7). Note that the mean vertical pathogen excursion shown in Fig. 7 does not reveal the frequent changes in the VPP. In general, variations of the VPP were restricted to the SML layer and spatially separated from the strongly stratified metalimnion where turbulent is greatly reduced. Consequently, the deepening of the SML caused the pathogens to be transported to greater depth and eventually to the depth of the intake initially located below the SML (Fig. 4g). Deepening of the SML occurred in response to enhanced vertical mixing induced by convective cooling and wind shear on a daily basis, thus, increasing the depth to which pathogens were dispersed. The vertical position of a given particle within the water column, in turn, determines the pathogen's survival and inactivation due to temperature and light.

3.4. Pathogen inactivation

The oocysts of *Cryptosporidium* are highly sensitive to solar radiation resulting in a high light inactivation in very clear waters and

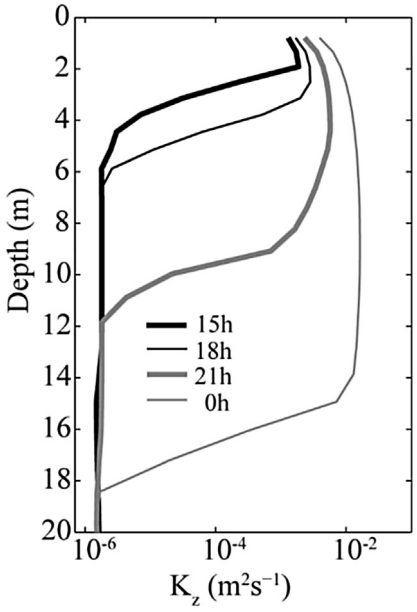

Fig. 6. Predicted vertical eddy diffusivity profiles at day 209 15 h (thick black), 18 h (thin black), 21 h (thick gray) and day 210 0 h (thin gray). Note the logarithmic scale.

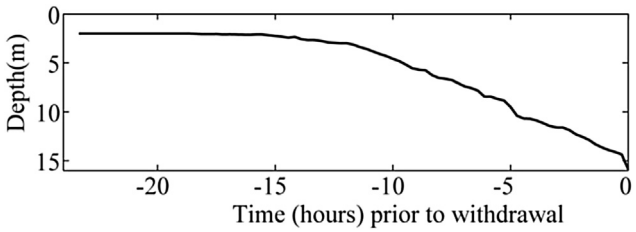

Fig. 7. Mean vertical pathogen excursion.

high UV flux, typical at Lake Tahoe. About 61% of those individuals that originated from shallow beach areas were inactivated due to solar radiation, while temperature inactivation occurred for less than 1% of individuals. The effect of radiation on the pathogen infectivity became evident in difference between the number of active (infectious) and inactive pathogens withdrawn during the morning hours (Fig. 4d). During the night, 95% of the pathogens withdrawn were infectious, as they traveled in absence of solar radiation during a large part of their trajectory.

Given incident short wave radiation values between 1 and 10^3 W m^{-2} observed for Lake Tahoe, a light attenuation coefficient k_{UV} of 0.15 m^{-1} and a 4-log inactivation dose ID_{99} of 10^3 Jm^{-2}, the time needed to inactivate 99.99% of pathogens ranges from O(1) min-O(1)d at 0.5 m depth (Fig. 8a). At 16 m depth, in contrast, inactivation time scale are one order of magnitude higher, ranging from O(10)min-O(10)d. The different inactivation time scale between 0.5 m and 16 m depth explains how pathogens could reach the intake during the early morning hours without being inactivated. Once the pathogens have reached a depth were UVR is significantly attenuated, they may continue traveling in spite of the increasing solar radiation reaching the free surface. The predicted time scales are in accordance with Connelly et al. (2007) who found that *Cryptosporidium* is inactivated by >99.99% during 10 h of light exposure during a mid-summer day at temperatures comparable to those found at Lake Tahoe (10°–20 °C). The predicted scales indicate that pathogens released in shallow water, where they are exposed to high solar radiation intensities, are inactivated within <O(1)d. The inactivation of pathogens is likely to occur within short periods of time as the hours of maximal bathing activity coincide with hours of maximal solar radiation (late morning until early evening). Consequently, the light dose received due to exposure to UVR would have to be low in order for pathogens to be infective when being withdrawn at the intake. Low light (UVR) doses can result from (i) short transport time scales due to short transport distance or high current velocities, and (ii) transport at times or depths of low light intensity.

Solar radiation is the main agent for pathogen inactivation with rates exceeding those of temperature inactivation or losses due to settling, in agreement with Hipsey et al. (2004). Daily losses due to temperature inactivation were of O(1)% (Fig. 8b) and losses due to settling were negligible. The importance of solar radiation for pathogen inactivation found is in contrast to other studies that did not consider the effect of solar radiation on pathogen infectivity (Anderson et al., 1998; Stewart et al., 2002) or those that considered settling to significantly reduce oocyst concentrations in the water column (Medema et al., 1998; Hawkins et al., 2000). Although alpine Lake Tahoe is characterized by high radiation intensities and high water clarity (i.e. low light attenuation with depth), a similar importance of solar inactivation for pathogen inactivation is expected to be found for other lakes or reservoirs (Hipsey et al., 2004).

4. Conclusions

- The risk of human water-borne pathogen originating from recreational beaches to enter drinking water intakes was evaluated using a novel and computationally efficient back-tracking technique. This technique allows to back-track individual pathogens from the water intake of concern towards their points of origin and evaluate their fate (inactivation) due to the environmental conditions (temperature and solar radiation) endured during their journeys.
- The risk of pathogens entering drinking water intakes is low (0.02%), but is not totally absent. The risk of pathogens entering water intakes is tightly linked to the stability of the water column, in particular, to the depth of the surface mixed layer. Fluctuation of the thermocline and the diurnal mixed layer, due to seasonal SML deepening and convective mixing at night, have been shown to expose the drinking water intake to surface water potentially containing human water-borne pathogens. Thus, the vertical position of the intake in relationship to the expected depth of the thermocline, its seasonal and daily variations, influences the risk of viable pathogens being withdrawn. An obvious outcome of this observation is that to absolutely minimize the risk of human pathogens from body-contact recreation being entrained, drinking water intakes should be located at a depth below the oscillation maximum of the summer SML depth. Such considerations would also need to take into account likely lake levels in the face of extreme drought events, during which the intake is closer to the water surface.
- Knowledge about daily variation of risk of pathogen withdrawal may help to schedule the times of water withdrawal. Thus, water companies could alternate between water withdrawal, during times of near-zero risk, and no withdrawal during times of elevated risk. Special care should be taken at the weekends and holidays when beach visitor density increases and hours of

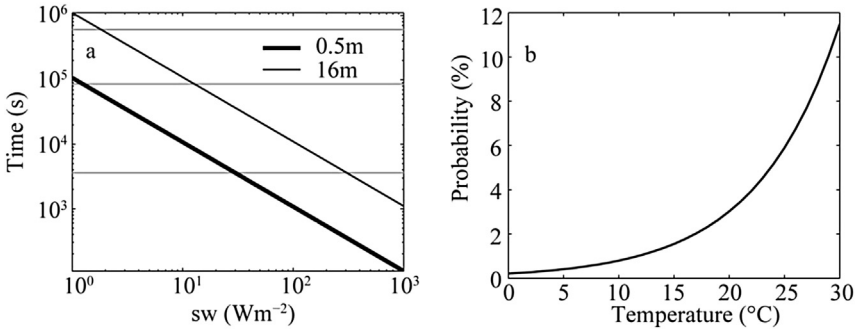

Fig. 8. Probability of *Cryptosporidium* inactivation. (a) Time scale for inactivation due to solar radiation at 0.5 m (thick black) and 16 m (thin black) depth. Gray horizontal lines in (a) mark 1 h, 1 d, and 1 week for reference. (b) Probability of inactivation due to water temperature following the inactivation rate proposed by Walker and Stedinger (1999).

beach activity may be extended. Also periods of strong wind forcing and, thus, strong current velocities may contain a potential risk of pathogens entering water intakes as transport times and exposure times to solar radiation decrease.

- The high sensitivity of pathogens, in particular of *Cryptosporidium*, to solar radiation is beneficial for the purpose of water disinfection and stresses the importance of water clarity. In clear lakes and reservoirs, solar radiation acts as a mechanism of natural water disinfection. Therefore, water clarity helps to improve water quality and, thus, its maintenance should be of high priority in lake and reservoir management, especially in drinking water sources.

Acknowledgments

Funding was provided by the Nevada Division of Environmental Protection. The parallel version of the hydrodynamic model was developed under the project CGL2008-06101 funded by the Spanish Government (*Ministerio de Innovación y Ciencia de España*). We would like to thank William Fleenor (UC Davis) and Simon Hook (NASA) for providing the meteorological data. We are grateful for the insightful comments of the anonymous reviewers.

References

Abdelzaher, A.M., Wright, M.E., Ortega, C., Solo-Gabriele, H.M., Miller, G., Elmir, S., Newman, X., Shih, P., Bonilla, J.A., Bonilla, T.D., Palmer, C.J., Scott, T., Lukasik, J., Harwood, V.J., McQuaig, S., Sinigalliano, C., Gidley, M., Plano, L.R.W., Zhu, X., Wang, J.D., Fleming, L.E., 2010. Presence of pathogens and indicator microbes at a non-point source subtropical recreational marine beach. Appl. Environ. Microbiol. 76, 724–732.

Acosta, M.C., Anguita, M., Fernández-Baldomero, F.J., Ramón, C.L., Schladow, S.G., Rueda, F.J., 2015. Evaluation of a nested-grid implementation for 3D finite-difference semi-implicit models. Environ. Model. Softw. 64, 241–261.

Anderson, M.A., Steward, Mic H., Yates, M.V., Gerba, C.P., 1998. Modeling the impact of body-contact recreation on pathogen concentration in a source drinking water reservoir. Water Res. 32 (1), 3293–3306.

Barnes, S.L., 1964. A technique for maximizing details in numerical weather map analysis. J. Appl. Meteorol. 3, 396–409.

Betancourt, W.Q., Rose, J.B., 2004. Drinking water treatment processes for removal of Cryptosporidium and Giardia. Vet. Parasitol. 126, 219–234.

Brookes, J.D., Antenucci, J., Hipsey, M., Burch, M.D., Ashbolt, N.J., Ferguson, C., 2004a. Fate and transport of pathogens in lakes and reservoirs. Environ. Int. 30, 741–759.

Brookes, J.D., Davies, C., Hipsey, M.R., Antenucci, J.P., 2004b. Association of *Cryptosporidium* with bovine faecel particles and implications for risk reduction by settling within water supply reservoirs. J. Water Health 4, 87–98.

Castanedo, S., Medina, R., 2002. Análisis de los modelos 3D para la simulación de flujo en aguas de transición. Ing. del agua 9, 467–481. http://dx.doi.org/10.4995/ia.2002.2628.

Center for Disease Control (CDC), 2000. Outbreak of gastroenteritis associated with an interactive water fountain at a beachside park — Florida, 1999. MMWR 49, 565–568.

Center for Disease Control (CDC), 2001. Notice to readers: responding to fecal accidents in disinfected swimming venues. MMWR 50, 416–417.

Connelly, S.J., Wolyniak, E.A., Williamson, C.E., Jellison, K.L., 2007. Artificial UV-B and solar radiation reduce in vitro infectivity of the human pathogen *Cryptosporidium parvum*. Environ. Sci. Technol. 41, 7101–7106.

Council of the European Communities, 1976. Council directive 76/160/EEC of 8 December 1975 concerning the quality of bathing water. Off. J. Eur. Communities L031, 1–7.

Coupe, S., Delabre, K., Pouillot, R., Houdart, S., Santillana-Hayat, M., Derouin, F., 2006. Detection of Cryptosporidium, Giardia and Enterocytozoon bieneusi in surface water, including recreational areas: a one-year prospective study. FEMS Immunol. Med. Microbiol. 47, 351–359.

Craik, S.A., Weldon, D., Finch, G.R., Bolton, J.R., Belosevic, M., 2001. Inactivation of Cryptosporidium parvum oocysts using medium- and low-pressure ultraviolet radiation. Water Res. 35, 1387–1398.

Craun, G.F., Calderon, R.L., Craun, M.F., 2005. Outbreaks associated with recreational water in the United States. Int. J. Environ. Health Res. 15, 243–262.

Dai, X., Boll, J., 2003. Evaluation of attachment of *Cryptosporidium parvum* and *Giardia lamblia* to soil particles. J. Environ. Qual. 32, 296–304.

Dai, X., Boll, J., 2006. Settling velocity of *Cryptosporidium parvum* and *Giardia lamblia*. Water Res. 40, 1321–1325. http://dx.doi.org/10.1016/j.watres.2006.01.027.

Dai, X., Boll, J., Hayes, M., Aston, D., 2004. Adhesion of Cryptosporidium parvum and Giardia lamblia to solid surface: the role of surface charge and hydrophobicity. Colloid Surf. B Biointerface 34, 259–263.

Farthing, M.J.G., 2000. Clinical aspects of human cryptosporidiosis. In: Petry, F., Karger, B. (Eds.), Cryptosporidiosis and Microsporidiosis. Contrib. Microbiol. 6, 50–74.

Farthing, M.J., 2006. Treatment options for the eradication of intestinal protozoa. Nat. Clin. Pract. Gastroenterol. Hepatol. 3, 436–445.

Fayer, R., 2004. Cryptosporidium: a water-borne zoonotic parasite. Vet. Parasitol. 126, 37–56.

Gallaher, M.M., Herdon, J., Nims, L., Sterling, C.R., Grabowski, D., Hull, H., 1989. Cryptosporidiosis and surface water. AJPH 79 (1), 39–42.

Gardner, J.V., Mayer, L.A., Hudges Clark, J.E., 1998. Cruise Report, RV Inland Surveyor Cruise IS-98: the Bathymetry of Lake Tahoe, California-Nevada, p. 28. U.S. Geological Survey Open-file Report 98–509. http://blt.wr.usgs.gov.

Gerba, C.P., 2000. Assessment of enteric pathogens shedding by bathers during recreational activity and its impact on water quality. Quant. Microbiol. 2, 55–68.

Gerba, C.P., 2002.

Graczyk, T.K., Sunderland, D., Tamang, L., Lucy, F.E., Breysee, P.N., 2007. Bather density and levels of *Cryptosporidium*, *Giardia*, and pathogenic microsporidian spores in recreational bathing water. Parasitol. Res. 101, 1729–1731.

Grant, R.H., Heisler, G.M., Gao, W., 1997. Ultraviolet sky radiance distribution of translucent overcast skies. Theor. Appl. Climatol. 58, 129–139.

Han, Y.-J., Holsen, T.M., Hopke, P.K., Yi, S.-M., 2005. Comparison between back-trajectory based modeling and lagrangian backward dispersion modeling for locating sources of reactive gaseous mercury. Environ. Sci. Technol. 39, 1715–1723.

Harwood, V.J., Levine, A.D., Scott, T.M., Chivukula, V., Lukasik, J., Farrah, S.R., Rose, J.B., 2005. Validity of the indicator organisms paradigm for pathogen reduction in reclaimed water and publick health protection. Appl. Environ. Microbiol. 71, 3163–3170.

Hawkins, P.R., Swanson, P., Warnecke, M., Shanker, S.R., Nicholson, C., 2000. Understanding the fate of *Cryptosporidium* and *Giardia* in storage reservoirs: a legacy of Sydney's water contamination incident. Aqua 49 (6), 289–306.

Hijnen, W., Beerendonk, E., Medema, G., 2006. Inactivation credit of UV radiation for viruses, bacteria and protozoan (oo)cysts in water: a review. Water Res. 40, 3–22.

Hipsey, M.R., Antenucci, J., Brookes, J.D., Burch, M.D., Regel, R.H., Linden, L., 2004. A three dimensional model of Cryptosporidium dynamics in lakes and reservoirs: a new tool for risk management. Int. J. River Basin Manag. 2 (3), 181–197.

Hoxie, N.J., Davis, J., Vergeront, J., Nashold, R., Blair, K., 1997. Cryptosporidiosis-associated mortality following a massive waterborne outbreak in Milwaukee, Wisconsin. Am. J. Public Health 87, 2032–2035.

Hoyer, A.B., Wittmann, M.E., Chandra, S., Schladow, S.G., Rueda, F.J., 2014. A 3D individual-based aquatic transport model for the assessment of the potential dispersal of planktonic larvae of an invasive bivalve. J. Environ. Manag. 145, 330–340.

Hoyer, A.B., Schladow, S.G., Rueda, F.J., 2015. Local dispersion of nonmotile invasive bivalve species by wind-driven lake currents. Limnol. Oceanogr. 6 (2), 446–462. http://dx.doi.org/10.1002/lno.10046.

Jellison, K.L., Hemond, H.F., Schauer, D.B., 2002. Sources and species of *Cryptosporidium* oocysts in the Wachusett reservoir watershed. Appl. Environ. Microb. 68, 569–575.

King, B.J., Monis, P.T., 2007. Critical processes affecting Cryptosporidium oocyst survival in the environment. Parasitology 134, 309–323.

King, B.J., Hoefel, D., Daminato, D.P., Fanok, S., Monis, P.T., 2008. Solar UV reduces *Cryptosporidium parvum* oocyst infectivity in environmental waters. J. Appl. Microbiol. 104, 1311–1323.

Largier, J., 2003. Considerations in estimating larval dispersal distances from oceanographic data. Ecol. Appl. 13 (1), S71–S89.

LeChevallier, M.W., Norton, W.D., Lee, R.G., 1991. *Giardia* and *Cryptosporidium* spp. in filtered drinking water supplies. Appl. Environ. Microbiol. 57 (9), 2617–2621.

MacKenzie, W.R., Hoxie, N.J., Proctor, M.E., Gradus, M.S., Blair, K.A., Peterson, D.E., Kazmierczak, J.J., Addiss, D.G., Fox, K.R., Rose, J.B., Davis, M.D., 1994. A massive outbreak in Milwaukee of Cryptosporidium infection transmitted through the public water supply. N. Engl. J. Med. 331, 161–167.

Masur, H., Kaplan, J.E., Holmes, K.K., 2002. Guidelines for preventing opportunistic infections among HIV-infected persons — 2002. Ann. Intern. Med. 137 (5), 435–478.

Medema, G.J., Schets, F.M., Teunis, P.F.M., Havelaar, A.H., 1998. Sedimentation of free and attached *Cryptosporidium* oocysts and Giaria cysts in water. Appl. Environ. Microbiol. 64 (11), 4460–4466.

Monis, P., King, B., Keegan, A., 2014. Removal and inactivation of *Cryptosporidium* from water. In: Cacciò, S.M., Widmer, G. (Eds.), Cryptosporidium: Parasite and Disease. Springer, pp. 515–552.

Morita, S., Namikoshi, A., Hirata, T., Oguma, K., Katayama, H., Ohgaki, S., Motoyama, N., Fijiwara, M., 2002. Efficacy of UV irradiation in inactivating *Cryptosporidium parvum* oocysts. Appl. Environ. Microbiol. 68, 5387–5393.

Nickols, K., Gaylord, B., Largier, J., 2012. The coastal boundary layer: predictable current structure decreases alongshore transport and alters scales of dispersal. MEPS 464, 17–35.

Ongerth, J.E., Pecoraro, J.P., 1996. Electrophoretic mobility of *Cryptosporidium parvum* and *Giardia lamblia* cysts. J. Environ. Eng. 122 (3), 228–231.

Rao, Y.R., Schwab, D.J., 2007. Transport and mixing between the coastal and offshore waters in the Great Lakes: a review. J. Gt. Lakes Res. 33, 202–218.

Reynolds, C.S., 1984. The Ecology of Freshwater Phytoplankton. Cambridge University Press, Cambridge.

Rochelle, P.A., Upton, S.J., Montelone, B.A., Woods, K., 2005. The response of Cryptosporidium parvum to UV light. Trends Parsitol. 21 (2), 81–87.

Rose, J.B., Gerba, C.P., Jakubowski, W., 1991. Survey of potable water-supplies for *Crytosporidium* and *Giardia*. Environ. Sci. Technol. 25, 1393–1400.
Rose, J.B., Huffmann, D.E., Gennaccaro, A., 2002. Risk and control of waterborne cryptosporidiosis. FEMS Microbiol. Rev. 26, 113–123.
Rose, K.C., Williamson, C.E., Schladow, S.G., Winder, M., Oris, J.T., 2009. Patterns of spatial and temporal variability of UV transparency in Lake Tahoe, California-Nevada. J. Geophys. Res. 114, G00D03.
Ross, O.N., Sharples, J., 2004. Recipe for 1-D Lagrangian particle tracking models in space-varying diffusivity. Limnol. Oceanogr. Methods 2, 289–302.
Rossignol, J., Kabil, S., El-Gohary, Y., Younis, A., 2006. Effect of nitozoxanide in diarrhea and enteritis caused by *Cryptosporidium* species. Clin. Gastroenterol. Hepatol. 4, 320–324.
Rueda, F.J., Schladow, S.G., Clark, J.F., 2008. Mechanisms of contaminant transport in a multi-basin lake. Ecol. Appl. 18, A27–A87.
Sherchand, J.B., 2012. Future emerging issues in waterborne diseases and microbial agents. J. Inst. Med. 34 (3), 1–3.
Shintani, T., de la Fuente, A., Niño, Y., Imberger, J., 2010. Generalization of the Wedderburn number: parameterizing upwelling in stratified lakes. Limnol. Oceanogr. 53 (3), 1377–1389. http://dx.doi.org/10.4319/lo.2010.55.3.1377.
Smith, H.V., Corcoran, G.D., 2004. New drugs and treatment for cryptosporidiosis. Curr. Opin. Infect. Dis. 17, 557–564.
Smith, P.E., 2006. A Semi-implicit, Three-dimensional Model for Estuarine Circulation. Open-file report 2006–1004. U.S. Department of the Interior. U.S. Geological Survey.
Standish-Lee, P., Loboschefsky, E., 2006. Protecting public health from the impact of body-contact recreation. Water Sci. Technol. 53, 201–207.
Stevens, C., Imberger, J., 1996. The initial response of a stratified lake to a surface shear stress. J. Fluid Mech. 312, 39–66.
Stewart, M.H., Yates, M.V., Anderson, M.A., Gerba, C.P., Rose, J.B., De Leon, R., Wolfe, R.L., 2002. Predicted public health consequences of body-contact recreation on a potable water reservoir. J. AWWA 94, 84–97.
Sunderland, D., Graczyk, T.K., Tamang, L., Breysse, P.N., 2007. Impact of bathers on levels of *Cryptosporidium parvum* oocysts and *Giardia lamblia* cysts in recreational beach waters. Water Res. 41, 348303489.
U.S. Environmental Protection Agency (USEPA), 1989. National primary drinking water regulations; infiltration and disinfection; turbidity; *Giardia lamblia*; viruses, Legionella, and heterotrophic bacteria. Fed. Reg. 54, 27486–27541.
U.S. Environmental Protection Agency (USEPA), 2002. Implementation Criteria for Ambient Water Quality Criteria for Bacteria. EPA-823-B-02–003. Office of Research and Development, Office of Water, U.S. Environmental Protection Agency, Washington, DC, USA.
Wade, T.J., Calderon, R.L., Sams, E., Beach, M., Brenner, K.P., Williams, A.H., Dufour, A.P., 2006. Rapidly measured indicators of recreational water quality are predictive of swimming-associated gastrointestinal illness. Environ. Health Perspect. 114, 24.
Walker, F.R., Stedinger, J.R., 1999. Fate and transport model of *Cryptosporidium*. J. Environ. Eng. 125 (4), 325–333.
World Health Organization, 2008. Guidelines for Drinking Water Quality, third ed., vol. 1. WHO, Geneva, Switzerland.
Wu, J., Rees, P., Storrer, S., Alderisio, K., Dorner, S., 2009. Fate and transport modeling of potential pathogens: the contribution from sediments. J. Am. Water Resour. Assoc. 45 (1), 35–44. http://dx.doi.org/10.111/j.1752-1688.2008.00287.x.
Yates, M.V., et al., 1997. The Impact of Body-contact Recreation in the Eastside Reservoir Project on (1) Pathogen Risk to Consumers and Recreators and (2) MTBE Contamination. Final report submitted to MMDSC.
Yoder, J.S., Blackburn, B.G., Craun, G.F., Hill, V., Levy, D.A., Chen, N., Lee, S.H., Calderon, R.L., Beach, M.J., 2004. Surveillance for waterborne-disease outbreaks associated with recreational water – United States, 2001–2002. MMWR Surveill. Summ. 53, 1–22.